Universidade de São Paulo

Biblioteca Digital da Produção Intelectual - BDPI

Sem comunidade WoS

2012

Particle Acceleration in Turbulence and Weakly Stochastic Reconnection

P H Y S I C A L R E V I E W L E T T E R S

Particle Acceleration in Turbulence and Weakly Stochastic Reconnection

Grzegorz Kowal[*] and Elisabete M. de Gouveia Dal Pino

Instituto de Astronomia, Geofísica e Ciências Atmosféricas, Universidade de São Paulo,
Rua do Matão, 1226 – Cidade Universitária, CEP 05508-090, São Paulo/SP, Brazil

A. Lazarian

Department of Astronomy, University of Wisconsin, 475 North Charter Street, Madison, Wisconsin 53706, USA

In this Letter we analyze the energy distribution evolution of test particles injected in three dimensional (3D) magnetohydrodynamic (MHD) simulations of different magnetic reconnection configurations. When considering a single Sweet-Parker topology, the particles accelerate predominantly through a first-order Fermi process, as predicted in [3] and demonstrated numerically in [8]. When turbulence is included within the current sheet, the acceleration rate is highly enhanced, because reconnection becomes fast and independent of resistivity [4,11] and allows the formation of a thick volume filled with multiple simultaneously reconnecting magnetic fluxes. Charged particles trapped within this volume suffer several head-on scatterings with the contracting magnetic fluctuations, which significantly increase the acceleration rate and results in a first-order Fermi process. For comparison, we also tested acceleration in MHD turbulence, where particles suffer collisions with approaching and receding magnetic irregularities, resulting in a reduced acceleration rate. We argue that the dominant acceleration mechanism approaches a second order Fermi process in this case.

Introduction.—Energetic particles are ubiquitous in astrophysical environments. While particle acceleration in shocks has been extensively explored (see [1,2] for reviews), an alternative and less investigated mechanism involves particle acceleration in magnetic reconnection sites. Magnetic reconnection may occur when two magnetic fluxes of opposite polarity encounter each other. In the presence of finite magnetic diffusivity the converging magnetic lines annihilate at the discontinuity surface and a current sheet forms there. Reference [3] proposed that an efficient first-order Fermi process can occur within a current sheet, where trapped charged particles may bounce back and forth several times and gain energy due to head-on collisions with the two converging magnetic fluxes incoming with the reconnection speed V_{rec}. They found that the particle energy gain after each round trip is $\Delta E/E \propto V_{rec}/c$. With a *fast* magnetic reconnection, like the one induced in the presence of turbulence [4], V_{rec} can be of the order of Alfvén speed V_A. Afterwards, [5] appealed to a similar process, but within a collisionless reconnection scenario. In their model, the acceleration is controlled by the contraction of two-dimensional (2D) loops due to firehose instability that arises in a particle-in-cell (PIC) domain (see also [6,7]).

In this Letter, we explore this issue by means of fully 3D MHD simulations of particle acceleration in magnetic reconnection domains. A preliminary study was performed in [8] where the analytical model of [3] was successfully tested. It was also shown that particle acceleration taking place in MHD reconnection domains without including

kinetic effects produces results similar to those found in collisionless PIC simulations [6]. This proved that the acceleration in reconnection regions is a universal process which is not determined by the details of the plasma physics and can work efficiently in collisional or collisionless gas, although energy and radiative losses due to the interactions of the accelerated particles with the surrounding plasma may be significant in some systems. Moreover, it has been shown that particle acceleration in 2D and 3D MHD reconnection behaves quite differently, which calls for focusing on realistic 3D geometries. In this work we study differences between energy distributions of test particles injected in 3D MHD reconnection sites with and without turbulence, corresponding to the Sweet-Parker [9,10] and Lazarian-Vishniac [4] configurations. For comparison, we also considered a pure turbulent environment.

Numerical simulations of reconnection and turbulence.—Magnetic reconnection and turbulence were modeled by solving the MHD equations numerically on a uniform mesh using a shock-capturing Godunov-type scheme based on the 2nd order spatial reconstruction and 2nd Runge-Kutta (RK) time integration with the HLLD Riemann solver and constrained transport (CT) integration of the induction equation to maintain the $\boldsymbol{\nabla} \cdot \boldsymbol{B} = 0$ constraint numerically (see [11,12]). The reconnection and turbulent models were performed in the same way as described in [11,12], by adopting an initial Harris current sheet in the reconnection models and uniform magnetic field in the turbulent model. We employed dimensionless equations, so that the velocity and magnetic field are

expressed in the fiducial Alfvén speed units (defined by the X component of the field and the unperturbed density $\rho_0 = 1$). For more details on the numerical setup, see [11,12].

Integration of particle trajectories.—In order to integrate the test particle trajectories we freeze in time a data cube obtained from the MHD models and inject 10,000 test particles in the domain with random initial positions and directions and with an initial thermal distribution. For each particle we solve the relativistic motion equation

$$\frac{d}{dt}(\gamma m \boldsymbol{u}) = q(\boldsymbol{E} + \boldsymbol{u} \times \boldsymbol{B}), \tag{1}$$

where m, q and $\boldsymbol{u}$ are the particle mass, electric charge, and velocity, respectively, $\boldsymbol{E}$ and $\boldsymbol{B}$ are the electric and magnetic fields, respectively, $\gamma \equiv (1 - u^2/c^2)^{-1}$ is the Lorentz factor, and c is the speed of light. The electric field $\boldsymbol{E}$ is taken from the MHD simulations:

$$\boldsymbol{E} = -\boldsymbol{v} \times \boldsymbol{B} + \eta \boldsymbol{J}, \tag{2}$$

where $\boldsymbol{v}$ is the plasma velocity, $\boldsymbol{J} \equiv \boldsymbol{\nabla} \times \boldsymbol{B}$ is the current density, and η is the Ohmic resistivity coefficient. We neglect the resistive term above since its effect on particle acceleration is negligible [8]. In the current studies we do not include the particle energy losses; thus particles can gain or loose energy only through the interactions with the moving magnetized plasma. The inclusion of radiative losses or back reaction on the plasma is planned for future studies, particularly with the incorporation of the kinetic effects. We note that since we are focusing on the acceleration process only, we consider very simple domains which represent only small periodic boxes of entire magnetic reconnection or turbulent sites. For this reason, the typical crossing time through the box of an injected thermal particle is very small and it has to re-enter the computational domain several times before gaining significant energy by multiple scatterings. Thus, whenever a particle reaches the box boundary it re-enters in the other side to continue scattering. We integrate Eq. (1) using the standard 4th order Runge-Kutta method with the adaptive time step with cubic (limited to constant near discontinuities) interpolation of the fields [8]. For convenience, we assume the speed of light to be $20V_A$, which defines our plasma in a non-relativistic regime, and the mean density is assumed to be 1 atomic mass unit per cubic centimeter, which is a fiducial value, e.g., of the interstellar medium (ISM) density. All times are expressed in units of the Alfvén time.

Acceleration in Sweet-Parker reconnection.—In the Sweet-Parker model [9,10] the reconnection speed is given by $V_{\text{rec}} \approx V_A S^{-1/2}$, where $S = LV_A/\eta$ is the Lundquist number. Because of the typical huge astrophysical sizes (L), S is also huge for Ohmic diffusivity values (e.g., for the ISM, $S \sim 10^{16}$). The Sweet-Parker reconnection is very slow, unless we use an artificially large diffusivity. In the model shown in the top panel of Fig. 1 we employed a diffusivity coefficient $\eta = 10^{-3}$ expressed in code units. This value, due to the numerical diffusivity, is several orders of magnitude larger than typical Ohmic diffusivity

in astrophysical environments, and makes the Sweet-Parker reconnection in the simulation efficient. The time evolution of the energy distribution for the accelerating particles is shown for this model in the top left panel of Fig. 1. Initially, the perpendicular acceleration dominates, because the volume in which we inject particles is much larger than the current sheet region (shown in the right panel of the same figure). The perpendicular acceleration, due to a drift of the magnetic flux, starts before the particles reach the reconnection region [8]. The distribution of particles does not change significantly until $t = 1.0$. Then, a rapid increase in energy by roughly four orders of magnitude appears for a fraction of particles. We observe a big gap between the energy levels before and after these acceleration events, which is also evident in the particle energy spectrum depicted in the embedded subplot of the same diagram. The events are spread in time because particles gain substantial energy at different moments when crossing the current sheet. The energy growth during this stage is exponential. This is a first-order Fermi acceleration process, as predicted in [3] and tested already in [8].

Around $t = 10$, we see a transition from an exponential to a power-law particle energy dependence with estimated index $\alpha \sim 1.1$ (see the upper plot of Fig. 1). A similar transition was also observed in [8]. In the plot we show the kinetic energy normalized by the proton rest mass, which is equivalent to $(\gamma - 1)$. The exponential acceleration stops right after the energy value 10^4 is reached, because the gyroradii exceed the thickness of the acceleration region. From this moment on the particles cannot be confined within this thickness and the first order Fermi process ceases. Further energy increase is due to a much slower drift acceleration (of the perpendicular component only) caused by the large scale magnetic fields gradients. The presence of a guide field allows the particles to accelerate in the parallel direction as well.

Although the Sweet-Parker model with an artificially enhanced resistivity results in a predominantly first-order Fermi acceleration, only a small fraction of the injected particles are trapped and efficiently accelerated in the current sheet (see the energy spectrum of the accelerated particles in the bottom right of Fig. 1), because the acceleration zone is very thin.

Acceleration in reconnection with turbulence.—Lazarian and Vishniac [4] proposed a model for fast reconnection that does not depend on the magnetic diffusivity (see also [13]). The model appeals to the ubiquitous astrophysical turbulence as a universal trigger of fast reconnection. The predictions of this model have been successfully tested in numerical simulations [11,12] which confirmed that the reconnection speed is of the order of the Alfvén speed. An important consequence of the fast reconnection by turbulent magnetic fields is the formation of a thick volume filled with small scale magnetic fluctuations. In order to test the acceleration of particles within
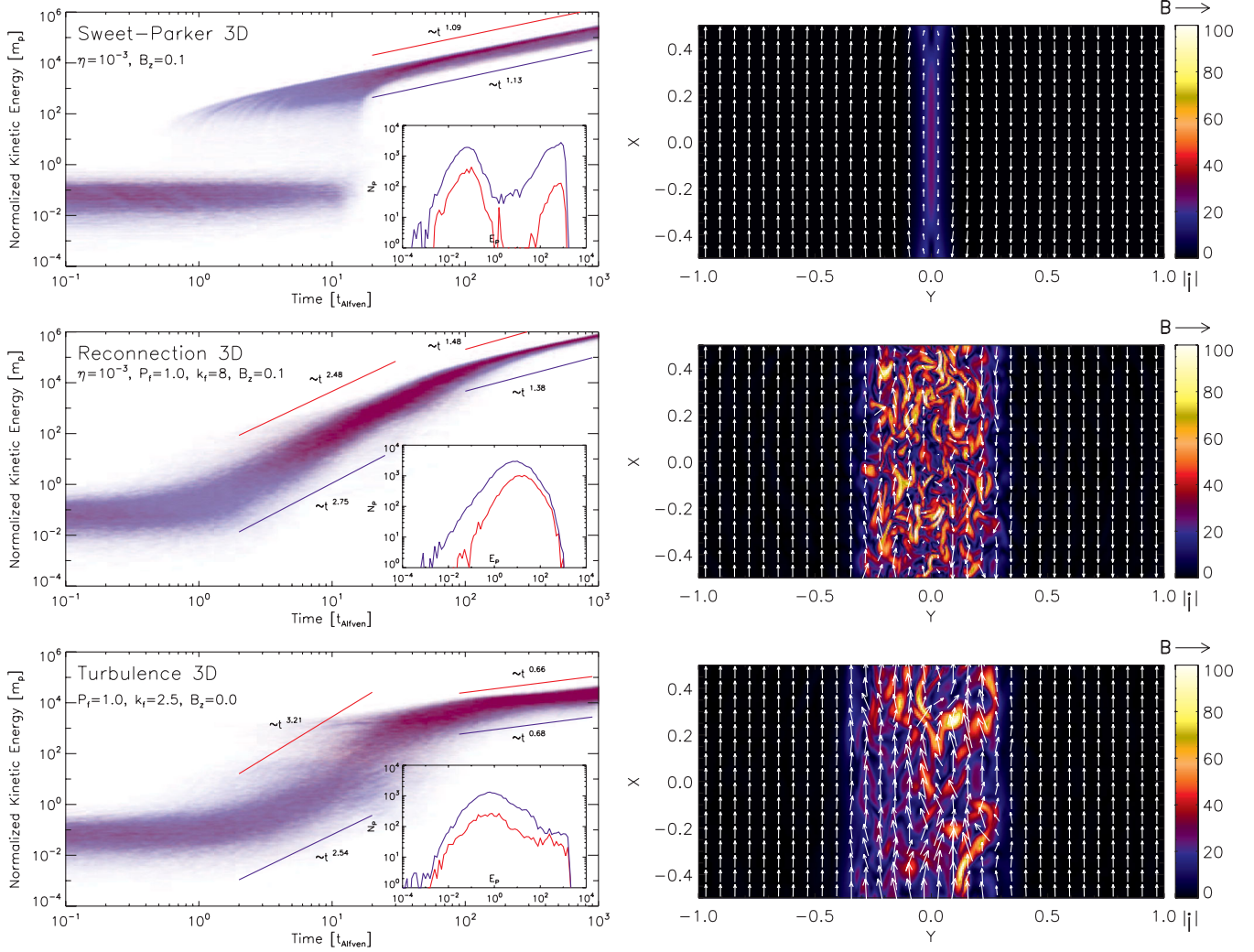
FIG. 1 (color).   Left column: Particle kinetic energy distributions for 10 000 protons injected in the Sweet-Parker reconnection (top), fast magnetic reconnection (middle), and purely turbulent (bottom) domains. The colors indicate which velocity component is accelerated (red or blue for parallel or perpendicular, respectively). The energy is normalized by the rest proton mass. Subplots show the particle energy distributions at $t = 5.0$. Right column: The exemplary XY cuts through the domain at $Z = 0$ of the absolute value of current density $|\vec{J}|$ overlapped with the magnetic vectors for the Sweet-Parker reconnection (top), fast reconnection (middle), and purely turbulent domains (bottom). Models with $B_{0z} = 0.1$, $\eta = 10^{-3}$, and the resolution $256 \times 512 \times 256$ for reconnection and $B_{0z} = 0.2$ and the resolution $128 \times 256 \times 128$ for the turbulent cases are shown.

such a domain, we introduced turbulence within a current sheet with a Sweet-Parker configuration (as described in the previous paragraph), then we followed the trajectories of 10,000 protons injected in this domain.

The middle left panel of Fig. 1 shows the evolution of the kinetic energy of the particles. After injection, a large fraction of test particles accelerate and the particle energy growth occurs earlier than in the Sweet-Parker case (see also the energy spectrum at $t = 5$ in the detail at the bottom right of the same diagram). This is explained by a combination of two effects: the presence of a large number of converging small scale current sheets, and the broadening of the acceleration region due to the turbulence. Here, we do not observe a gap seen in the Sweet-Parker reconnection, because particles are continually accelerated by en-

counters with several small and intermediate scale current sheets randomly distributed in the thick volume. The acceleration process is clearly still a first-order Fermi process, as in the Sweet-Parker case, but more efficient as it involves a larger number of particles, since the size of the acceleration zone and the number of scatterers have been naturally increased by the presence of turbulence. Moreover, the reconnection speed, which in this case is independent of resistivity [4,11] and determines the velocity at which the current sheets scatter particles, has been naturally increased as well (i.e., $V_{\rm rec} \sim V_A$).

During this stage α is in the range 2.48–2.75. Then, like in the laminar case, the protons accelerate at smaller rates after reaching an energy level $\sim 10^4$, because the thickness of the acceleration region (and of the plasma scattering centers)

becomes smaller than their Larmor radii. This, however, occurs later than in the previous case (around $t = 100$).

Acceleration in pure turbulence.—For comparison, in the bottom left panel of Fig. 1 we show the kinetic energy evolution of accelerated particles in a domain with turbulence injected in an initially uniform large scale field. In this domain the acceleration is less efficient at the beginning and a much smaller fraction of particles are accelerated than in the reconnection case. The increase in the acceleration rate (with $\alpha = 2.54$–3.21) is partly due to constraints of the computational domain. We cannot inject turbulence at scales larger than the size of the box. As a consequence, an undesired converging flow arises in the direction perpendicular to the mean field due to pseudo-Alfvén waves compressing the field in the region of turbulent injection and open boundary conditions. This enhances the acceleration rate for particles with Larmor radii approaching the turbulent injection scale. After reaching an energy level of about 10^4 proton mass, this acceleration is significantly suppressed and α drops down to ~ 0.67. In the model with fast reconnection the presence of the large scale current sheet provides the converging flow. This flow brings scattering centers allowing a continuous growth of the particle energy until the saturation level. In pure turbulence, the absence of a converging flow results in a random particle scattering on approaching and receding small scale current sheets (although at a smaller rate), so that the overall acceleration is a second-order Fermi process. This point still requires further studies, as reconnection layers in pure turbulence can be responsible for first-order Fermi acceleration of low energy particles. As before, the rapid transition to smaller acceleration rate occurs when the particle gyroradius reaches the size of the turbulent domain and its irregularities (around $t = 10$).

We note that we have neglected here the time evolution of the MHD environment in order to make this model comparable with the two presented in previous paragraphs. In this model, however, the electric field arising from slow modes (betatron acceleration) can contribute to the acceleration process as well. In the incompressible limit, a particle feels an average electric field $\bar{\mathcal{E}} \propto -\int (\boldsymbol{B}_0 \cdot \boldsymbol{\nabla}) \boldsymbol{v}_l \cdot d\boldsymbol{s}$ during one gyrorotation, where $\boldsymbol{B}_0$ is the local mean field, $\mathbf{v}_l$ is the velocity in an eddy of size l, and $d\boldsymbol{s}$ is the infinitesimal area element vector [14]. This integral is non-zero for slow modes and has maximum amplitude when $l \sim r_g$ [see Eq. (47) in [14]]. Still, if the particle distribution is isotropic, this term is canceled by adiabatic gain or loss in parallel directions, as shown [14]. An example distribution for $t = 5$ of the turbulent model in Fig. 1 (subplot in the bottom left panel) shows the anisotropy at this stage. Therefore, our results for this model might be incorrect by a factor of 2, since the betatron term $\partial \boldsymbol{B}/\partial t$ contributes as much as the electric field in the second order process. In the forthcoming studies when considering more realistic non-steady environments we plan to use data cubes varying in time.

Conclusions.—In this letter we investigated particle acceleration in 3D MHD domains of magnetic reconnection. We found that the presence of turbulence significantly increases the acceleration rate in a first-order Fermi process as predicted in [3]. The particles trapped within the current sheet suffer several head-on scatterings with the contracting magnetic fluctuations in the thick volume. In the Sweet-Parker model, where the reconnection speed was artificially large due to numerical magnetic diffusivity, the acceleration rate is slightly smaller because of a thinner current sheet. This is still a first-order Fermi process, however. For comparison, we have also investigated the acceleration in a pure 3D turbulence, where the particles with gyroradii smaller than the injection scale accelerate through a second-order Fermi process.

In summary, we have shown that the acceleration within reconnection sites, especially in the presence of turbulence, work in both collisional and collisionless environments. In the collisional case, however, only the injected particles with Larmor radii near the MHD scales are effectively accelerated. This injection problem can be solved using hybrid codes which can resolve both kinetic and MHD scales. In order to check if this mechanism can be powerful enough not only in the solar corona and wind or the Earth magnetotail, but also in relativistic environments like the surroundings of black holes or accretion disks and jet launching regions of AGNs and GRBs, as suggested in the literature, further studies of the present model in the relativistic MHD regime are required. Our results also call for further extensive work on the CR acceleration in magnetic reconnection sites with the inclusion of relevant loss mechanisms of CRs in order to assess the importance of this acceleration mechanism in comparison to other processes (e.g., diffusive shock acceleration), and to reproduce the observed light curves of the sources.

*kowal@astro.iag.usp.br

[1] M. A. Malkov and L. O'C Drury, Rep. Prog. Phys. **64**, 429 (2001).

[2] D. B. Melrose, in *Encyclopedia of Complexity and Systems Science*, edited by R. Meyers (Springer, New York, 2009).

[3] E. M. de Gouveia Dal Pino and A. Lazarian, Astron. Astrophys. **441,** 845 (2005).

[4] A. Lazarian and E. T. Vishniac, Astrophys. J. **517,** 700 (1999).

[5] J. F. Drake, M. Swisdak, K. M. Schoeffler, B. N. Rogers, and S. Kobayashi, Geophys. Res. Lett. **33,** 13105 (2006).

[6] J. F. Drake, M. Opher, M. Swisdak, and J. N. Chamoun, Astrophys. J. **709,** 963 (2010).

[7] Y. Lyubarsky and M. Liverts, Astrophys. J. **682,** 1436 (2008).

[8] G. Kowal, E. M. de Gouveia Dal Pino, and A. Lazarian, Astrophys. J. **735,** 102 (2011).

[9] E. N. Parker, J. Geophys. Res. **62,** 509 (1957).

[10] P. A. Sweet, in *Conference Proceedings of the IAU Symposium 6, Electromagnetic Phenomena in Cosmical Physics*, edited by B. Lehnert (Cambridge University Press, Cambridge, U.K., 1958), p. 123.

[11] G. Kowal, A. Lazarian, E. T. Vishniac, and K. Otmianowska-Mazur, Astrophys. J. **700,** 63 (2009).

[12] G. Kowal, A. Lazarian, E. T. Vishniac, and K. Otmianowska-Mazur, Nonlinear Processes Geophys. **19,** 297 (2012).

[13] G. L. Eyink, A. Lazarian, and E. T. Vishniac, Astrophys. J. **743,** 51 (2011).

[14] J. Cho and A. Lazarian, Astrophys. J. **638,** 811 (2006).